

Broadband optical chaos for stimulated Brillouin scattering suppression in power over fiber

Xuelel Fu,¹ Sze-Chun Chan,^{1,*} Qing Liu,¹ and Kenneth Kin-Yip Wong²

¹Department of Electronic Engineering, City University of Hong Kong, Hong Kong, China

²Department of Electrical and Electronic Engineering, University of Hong Kong, Hong Kong, China

*Corresponding author: scchan@cityu.edu.hk

Received 2 March 2011; revised 28 June 2011; accepted 5 July 2011;
posted 11 July 2011 (Doc. ID 143478); published 21 July 2011

Broadband chaos generated in an optically injected semiconductor laser is applied for power-over-fiber transmission. By varying the injection power, period-one oscillation, period-two oscillation, and chaotic oscillation are observed in the injected slave laser, indicating a period-doubling route to chaos. Compared to the free-running output of the laser, its chaotic output has a drastically increased signal bandwidth, which leads to a 19 dB increase of the stimulated Brillouin scattering threshold. Using a chaos of 5.2 GHz bandwidth, a maximum optical power of 27 dBm is obtained after 20 km transmission over fiber, which is applicable to optically powering some advanced communication networks. The approach uses the inherent nonlinear laser dynamics, which requires no modulation electronics or microwave signal sources. © 2011 Optical Society of America

OCIS codes: 140.5960, 140.3520, 140.1540, 290.5900.

1. Introduction

Power over fiber (PoF) is a technique that uses optical fiber for power distribution. In a PoF system, optical power generated by a high-power light source is coupled into an optical fiber and transmitted to the remote site for optoelectronic conversion using photovoltaics (PVs). Compared to traditional copper-wire power supply systems, PoF systems provide excellent isolation, low distributed loss, and immunity to electromagnetic noise. With the advances of low-power devices, PoF has found applications in sensor networks, data links in high-voltage environments, and integration with the currently existing fiber communication networks and radio-over-fiber systems [1–5]. Although multimode fibers are often applied for PoF, single-mode fibers are sometimes preferred. The main advantage of single-mode fibers for PoF is their relatively low bending loss [6]. Single-mode fibers are also compatible with most deployed high-speed data networks and sensing devices [1,2].

The key limitation on the power transfer capacity of single-mode fibers is caused by stimulated Brillouin scattering (SBS). This nonlinear optical process generates a backward-propagating Stokes wave as a reflection that limits the net incident power at the input end to the SBS threshold [7–12]:

$$P_p^{\text{th}} = \left(1 + \frac{\Delta\nu_p}{\Delta f_B}\right) \cdot \frac{\ln G_B^{\text{th}} A_{\text{eff}} K}{\tilde{g}_{B0}^{\text{max}} l_{\text{eff}}}, \quad (1)$$

where Δf_B is the FWHM linewidth of the Brillouin gain spectrum, $\Delta\nu_p$ is the FWHM linewidth of the pump wave, G_B^{th} is the threshold amplification factor, A_{eff} is the effective mode area, $\tilde{g}_{B0}^{\text{max}}$ is the peak Brillouin gain factor for an idealized cw pump, $l_{\text{eff}} = (1 - \exp(-\alpha l))/\alpha$ is the effective length of the fiber of physical length l and attenuation α , and K is the polarization factor that accounts for polarization scrambling in typical single-mode fibers with residual fluctuating birefringence. Both the gain and the pump line shapes are assumed to be Lorentzian.

Once a fiber is chosen, the only way to raise P_p^{th} is to increase the pump wave linewidth $\Delta\nu_p$. A possibility is to employ high-power multimode laser diodes

0003-6935/11/250E92-05\$15.00/0
© 2011 Optical Society of America

as the light source [13]. However, the coupling loss into the fiber is large for multitransverse mode lasers. The multilongitudinal mode emission also takes up a large wavelength band, which causes difficulties multiplexing with data. A recent solution employed a single-mode laser that was modulated externally and amplified optically [14,15]. The method used external modulators together with high-speed driving electronics to broaden $\Delta\nu_p$. Related methods often require extra dithering electronics, multitone microwave sources, high-speed pseudorandom bit generators, or strongly amplified microwave noise sources [16,17].

In this paper, broadband optical chaos generated from a single-mode semiconductor laser using optical injection is applied for PoF. A significant increment in the bandwidth $\Delta\nu_p$ of chaos, as compared to that of the cw output from the free-running laser, drastically raises the SBS threshold and, thus, increases the maximum power deliverable over fibers. An increment of the SBS threshold by 19 dB is achieved and is comparable to that reported using noisy external modulation [17]. Moreover, since chaotic oscillation is part of the inherent laser nonlinear dynamics [18–21], our approach requires no external modulators, dithering circuitries, or high-speed electronics. The optical spectrum generated from the chaotic single-mode laser is continuous, which leads to better bandwidth efficiency as compared to conventional PoF using multimode lasers [13].

2. Experimental Setup

Figure 1 shows the schematic of the setup. The lasers used are distributed-feedback lasers (Mitsubishi ML920T43S-01) emitting at 1548 nm. Light from the master laser is injected into the slave laser through a free-space optical circulator, which ensures unidirectional injection. The circulator is arranged such that the polarizations of the injection and the slave laser are the same, thereby minimizing the injection power required to generate chaos [20]. The master laser is biased at 133.4 mA and temperature stabilized at 18.00 °C, while the slave laser is biased at 40.0 mA and temperature stabilized at 27.00 °C. Under this operating condition, the detuning frequency of the master laser from the slave laser is 11.0 GHz. The injection power can be tuned by adjusting a

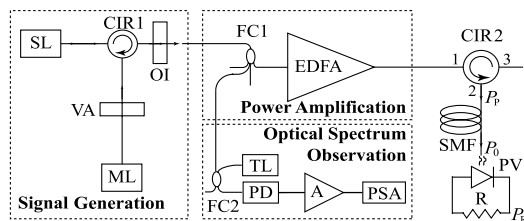


Fig. 1. Schematic of PoF transmission using optical chaos. ML, master laser; SL, slave laser; VA, variable attenuator; CIR, circulator; OI, optical isolator; FC, coupler; EDFA, erbium-doped fiber amplifier; SMF, single-mode fiber; PV, photovoltaic converter; R, resistor; TL, tunable laser; PD, photodetector; A, microwave amplifier; PSA, power spectrum analyzer.

variable attenuator. The slave laser has a relaxation resonance frequency of about 11 GHz. The output power is about 10 mW irrespective of the dynamics. Its threshold current is 9 mA. An optical isolator is adopted to prevent any backreflection.

The output after the optical isolator is coupled to a fiber coupler. One branch is directed to an erbium-doped fiber amplifier (EDFA, consisting of cascading Amonics AEDFA-23-B-FA and IPG Photonics EAR-10k-C), which can boost the optical power up to 36 dBm. A fiber-based optical circulator is employed to protect the EDFA from any possible reflected power. Single-mode fibers (Corning SMF-28e+) of lengths $l = 5, 10, 15,$ and 20 km are adopted to demonstrate long-distance power transmission. The fibers have attenuation $\alpha = 0.046 \text{ km}^{-1}$ and Brillouin linewidth $\Delta f_B = 25 \text{ MHz}$ [22]. At the output end of the fiber, electrical power is obtained through optoelectronic conversion using a PV converter (JDSU 9LC0097), which drives a load resistor of 353 Ω . The resistance is optimized for maximum conversion efficiency.

Since traditional optical spectrum analyzers cannot provide a fine enough frequency resolution, a specially constructed system is applied for optical spectrum observation. As shown in Fig. 1, a branch of the generated signal is combined with a narrow-linewidth cw emission from a tunable laser (HP 8168A) by a 3 dB fiber coupler. The wavelength of the tunable laser is fixed at 0.03 nm shorter than that of the master laser. The beat signal is then detected by a 43 GHz photodetector (Newport AD-10ir), amplified by 40 dB using two cascaded microwave amplifiers (HP 83006A and HP 83017A), and monitored on a 26.5 GHz power spectrum analyzer (Agilent N9010A).

3. Experimental Results

The optical spectrum from the slave laser is obtained and plotted in Fig. 2. The frequency axis is offset to the free-running frequency of the slave laser. The arrows indicate regeneration of the optical injection. By varying the injection power, different nonlinear dynamical states are observed from the slave laser. When the laser is free-running in Fig. 2(a), it emits single-frequency cw light. The linewidth is measured to be $\Delta\nu_p = 5 \text{ MHz}$. When the injection power is 0.05 mW, as in Fig. 2(b), the slave laser is forced into period-one oscillation, generating two components separated by 11.1 GHz. When the injection power is increased to 0.21 mW in Fig. 2(c), period-two oscillation is observed with generation of a subharmonic through period-doubling bifurcation. When the injection power increases to 0.31 mW in Fig. 2(d), optical chaos is clearly observed through a period-doubling route to chaos [18]. The spectrum shows significant broadening of signal bandwidth due to chaotic oscillation. As an estimation, by fitting the chaotic spectrum to a Lorentzian function, the linewidth of the signal is estimated to be $\Delta\nu_p = 5.2 \text{ GHz}$, which is much broader than the Brillouin linewidth. It is

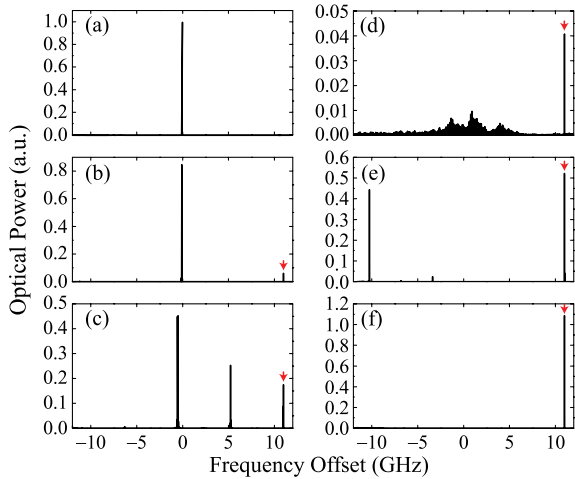


Fig. 2. (Color online) Optical spectra from the slave laser in the (a) free-running state, (b) period-one state, (c) period-two state, (d) chaotic state, (e) period-one state, and (f) stable-locking state, where the injection power is 0, 0.05, 0.21, 0.31, 3.78, and 23.6 mW, respectively. The injection detuning frequency is kept at 11.0 GHz, as the arrows indicate.

important to note that the regeneration is only 0.04 as strong as the free-running emission in Fig. 2(a). Most of the power in Fig. 2(d) is carried by the broadband chaos. The chaotic spectrum remains unchanged as long as the bias currents and the temperatures of the lasers are kept constant. When the injection is increased to 3.78 mW in Fig. 2(e), the slave laser goes back to period-one oscillation at a different frequency separation of 21.2 GHz. When the injection is 23.6 mW in Fig. 2(f), the slave laser is finally stably locked by the master laser [20]. In the following, the chaotic state in Fig. 2(d) is applied for PoF, which is compared with the performance of the cw emission from the free-running state in Fig. 2(a).

The output optical power P_0 after PoF transmission is plotted against the input power P_p in Fig. 3 with different fiber lengths. The results using the chaotic and the free-running states are respectively obtained as closed and open symbols for comparison. For the free-running state, the output power quickly

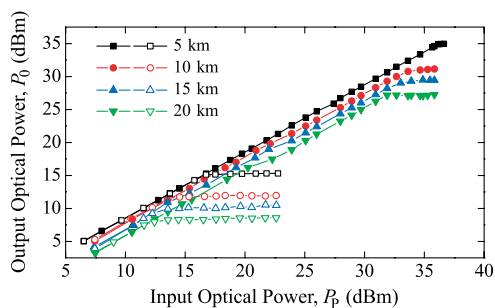


Fig. 3. (Color online) Output optical power versus input optical power for transmission over fibers. The fiber lengths are indicated by the legends. The open and closed symbols are obtained when the slave laser is in the free-running state and the chaotic state, respectively. For each curve, the output power saturates because of SBS reflection.

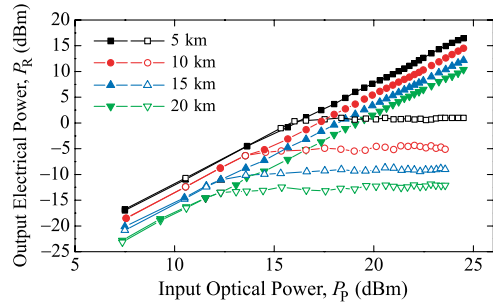


Fig. 4. (Color online) Output electrical power versus input optical power for transmission over fibers. The fiber lengths are indicated by the legends. The open and closed symbols are obtained when the slave laser is in the free-running state and the chaotic state, respectively.

saturates due to SBS, which is confirmed by monitoring the spectrum of the reflected signal from the fiber. For the chaotic state, the saturated power is significantly raised due to the broadened linewidth. Taking 20 km transmission as an example, the output optical power is saturated at 8.6 dBm for the free-running state, while the saturated power is greatly increased to 27 dBm using the chaotic state.

Moreover, Fig. 4 shows the associated electrical power P_R after optoelectronic conversion using the PV converter for demonstration. The performance of the PV converter limits the input power to only 24.5 dBm in order to prevent damage. Nonetheless, the electrical power obtained over a 5 km fiber using the free-running state saturates at 0.8 dBm due to SBS, while at least 16.4 dBm of electrical power is obtained using the chaotic state. This electrical power level is only limited by the PV converter used, but it is already adequate for powering some advanced remote units [4].

To further characterize the system, the saturated output optical power for the free-running and chaotic states is plotted in Fig. 5. The data points are fit to $\exp(-\alpha l)P_p^{\text{th}}$ using Eq. (1). The saturated power for the chaotic state increases by 19 dB as compared to the free-running state. The increment is a bit less than the estimated 22 dB from the measurements of linewidths $\Delta\nu_p$ in Fig. 2. This is possibly due to over-estimation of the linewidth of the chaotic signal when fitting to a Lorentzian function. In the experiments,

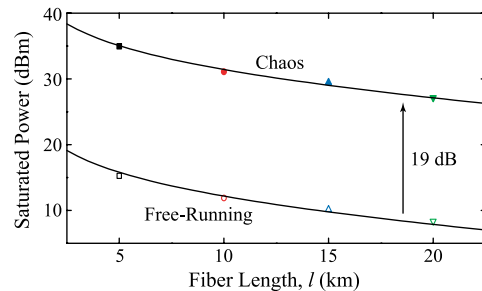


Fig. 5. (Color online) Saturated output optical power versus fiber length. The open and closed symbols are obtained when the slave laser is in the free-running state and the chaotic state, respectively.

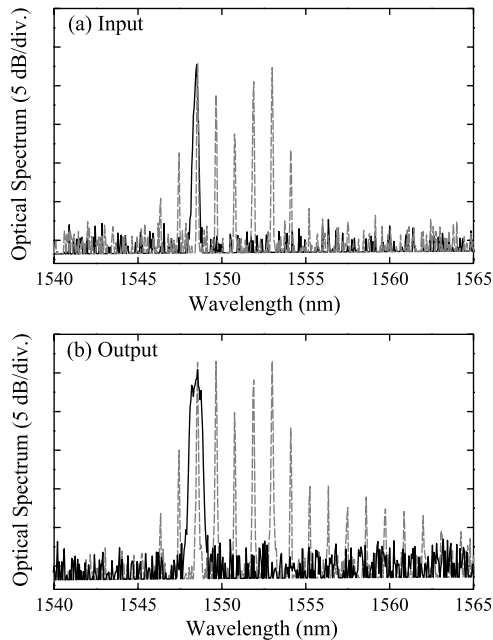


Fig. 6. Optical spectra measured (a) at the input to the EDFA and (b) at the output after PoF transmission. The solid curves are obtained when the optically injected single-mode laser is in the chaotic state. The dashed curves show the spectra obtained when the laser is replaced by a cw multilongitudinal mode laser without optical injection.

the saturated power does not depend on the state of polarization at the input of the fiber, which is due to polarization scrambling by residual fluctuating birefringence in the fiber [10].

4. Discussion

When compared to a conventional cw multilongitudinal mode laser, the chaotic single-mode laser is more bandwidth efficient. In Fig. 6, the solid and dashed curves are the optical spectra from the chaotic single-mode laser under optical injection and from a cw multimode laser without optical injection, respectively. Figure 6(a) shows the spectra measured at the input to the EDFA. Chaotic emission from the single-mode laser is concentrated at a single peak at about 1548 nm, while cw emission from the multimode laser is distributed over several peaks and occupies a wide bandwidth. Furthermore, the signals are transmitted over fiber for 20 km after being amplified by the EDFA to 31 dBm, which is below the SBS thresholds for both signals. Because of Kerr nonlinearity, spectral broadening for both signals is observed, as Fig. 6(b) shows. The discrete peaks of the dashed curve from the multimode laser are frequency mixed and result in a significant overall broadening to about 20 nm. By contrast, the solid curve for the chaotic single-mode laser is only slightly broadened, where the measured 20 dB bandwidth is just about 1 nm. Thus, the smaller overall bandwidth of the chaotic single-mode laser is attributed to its continuous spectrum centered at a single mode.

5. Conclusion

Optical chaos generated by optically injecting a semiconductor laser is applied for suppressing SBS in PoF. Because of the significantly increased signal bandwidth of the chaotic state, the saturated power for PoF is increased by 19 dB. A maximum optical power of 27 dBm is received after 20 km transmission. The approach uses the inherent nonlinear laser dynamics, which requires no modulation electronics or microwave signal sources. It is a promising candidate for optically powered sensing and communication networks. Chaos generation using simplified methods like optical feedback can also be considered.

The work described in this paper was fully supported by a grant from City University of Hong Kong (Project No. 7002448) and a grant from the Research Grant Council of Hong Kong, China (Project No. CityU 111210).

References

1. M. Roeger, G. Boettger, M. Dreschmann, C. Klamouris, M. Huebner, A. W. Bett, J. Becker, W. Freude, and J. Leuthold, "Optically powered fiber networks," *Opt. Express* **16**, 21821–21834 (2008).
2. Y. Tanaka, T. Shioda, T. Kurokawa, J. Oka, K. Ueta, and T. Fukuoka, "Power line monitoring system using fiber optic power supply," *Opt. Rev.* **16**, 257–261 (2009).
3. G. Boettger, M. Dreschmann, C. Klamouris, M. Huebner, M. Roeger, A. W. Bett, T. Kueng, J. Becker, W. Freude, and J. Leuthold, "An optically powered video camera link," *IEEE Photon. Technol. Lett.* **20**, 39–41 (2008).
4. D. Wake, A. Nkansah, and N. Gomes, "Optical powering of remote units for radio over fiber links," in *IEEE International Topical Meeting on Microwave Photonics* (IEEE, 2007), pp. 29–32.
5. D. Wake, A. Nkansah, N. J. Gomes, C. Lethien, C. Sion, and J.-P. Vilcot, "Optically powered remote units for radio-over-fiber systems," *J. Lightwave Technol.* **26**, 2484–2491 (2008).
6. T. C. Banwell, R. C. Estes, L. A. Reith, P. W. Shumate, Jr., and E. M. Vogel, "Powering the fiber loop optically—a cost analysis," *J. Lightwave Technol.* **11**, 481–494 (1993).
7. E. P. Ippen and R. H. Stolen, "Stimulated Brillouin scattering in optical fibers," *Appl. Phys. Lett.* **21**, 539–541 (1972).
8. J. M. Liu, *Photonic Devices* (Cambridge University, 2005).
9. A. B. Ruffin, M. J. Li, X. Chen, A. Kobayakov, and F. Annunziata, "Brillouin gain analysis for fibers with different refractive indices," *Opt. Lett.* **30**, 3123–3125 (2005).
10. R. H. Stolen, "Polarization effects in fiber Raman and Brillouin lasers," *IEEE J. Quantum Electron.* **15**, 1157–1160 (1979).
11. Y. Aoki, K. Tajima, and I. Mito, "Input power limits of single-mode optical fibers due to stimulated Brillouin scattering in optical communication systems," *J. Lightwave Technol.* **6**, 710–719 (1988).
12. M. O. van Deventer and A. J. Boot, "Polarization properties of stimulated Brillouin scattering in single-mode fibers," *J. Lightwave Technol.* **12**, 585–590 (1994).
13. H. Miyakawa, Y. Tanaka, and T. Kurokawa, "Design approaches to power-over-optical local-area-network systems," *Appl. Opt.* **43**, 1379–1389 (2004).
14. S. Yang, X. Xu, Y. Zhou, K. K. Y. Cheung, and K. K. Y. Wong, "Continuous-wave single-longitudinal-mode fiber-optical parametric oscillator with reduced pump threshold," *IEEE Photon. Technol. Lett.* **21**, 1870–1872 (2009).

15. X. Xu, K. K. Y. Cheung, S. Yang, Y. Liang, T. I. Yuk, and K. K. Y. Wong, "Optically powered WDM signal transmission system with distributed parametric amplification," *IEEE Photon. Technol. Lett.* **22**, 1232–1234 (2010).
16. T. Torounidis, B. E. Olsson, H. Sunnerud, M. Karlsson, and P. A. Andrekson, "Fiber-optic parametric amplifier in a loop mirror configuration," *IEEE Photon. Technol. Lett.* **17**, 321–323 (2005).
17. J. B. Coles, B. P. P. Kuo, N. Alic, S. Moro, C. S. Bres, J. M. Chavez Boggio, P. A. Andrekson, M. Karlsson, and S. Radic, "Bandwidth-efficient phase modulation techniques for stimulated Brillouin scattering suppression in fiber optic parametric amplifiers," *Opt. Express* **18**, 18138–18150 (2010).
18. T. B. Simpson, J. M. Liu, A. Gavrielides, V. Kovanis, and P. M. Alsing, "Period-doubling route to chaos in a semiconductor laser subject to optical injection," *Appl. Phys. Lett.* **64**, 3539–3541 (1994).
19. F. Y. Lin and J. M. Liu, "Harmonic frequency locking in a semiconductor laser with delayed negative optoelectronic feedback," *Appl. Phys. Lett.* **81**, 3128–3130 (2002).
20. S. C. Chan, S. K. Hwang, and J. M. Liu, "Period-one oscillation for photonic microwave transmission using an optically injected semiconductor laser," *Opt. Express* **15**, 14921–14935 (2007).
21. Y. Takeuchi, R. Shogenji, and J. Ohtsubo, "Chaotic dynamics in semiconductor lasers subjected to polarization-rotated optical feedback," *Appl. Phys. Lett.* **93**, 181105 (2008).
22. A. Kobaykov, M. Sauer, and D. Chowdhury, "Stimulated Brillouin scattering in optical fibers," *Adv. Opt. Photon.* **2**, 1–59 (2010).